PROCEEDINGS OF SCIENCE

Neutral pion bumps in the TeV spectra of X-ray flaring blazars

Maria Petropoulou,[a,b,*] **Apostolos Mastichiadis,**[a] **David Paneque**[c] **and Josefa Becerra González**[d,e]

[a] *Department of Physics, National and Kapodistrian University of Athens*
University Campus, Zografos, GR 15783, Athens, Greece
[b] *Institute of Accelerating Systems & Applications*
University Campus Zografos, GR 15783, Athens, Greece
[c] *Max-Planck-Institut für Physik, 80805, München, Germany*
[d] *Inst. de Astrofísica de Canarias, 38200 La Laguna, Spain*
[e] *Universidad de La Laguna, Dpto. Astrofísica, 38206 La Laguna, Tenerife, Spain*

E-mail: mpetropo@phys.uoa.gr

Very high-energy (VHE, $E > 100$ GeV) observations of blazar Mrk 501 with MAGIC in 2014 have revealed an unusual narrow spectral feature at ~ 3 TeV during an extreme **X-ray flare**. The one-zone synchrotron-self Compton scenario, widely used in blazar broadband spectral modeling, fails to explain the narrow TeV component. Motivated by this rare observation, we propose an alternative model where narrow features in VHE blazar spectra result from the decay of neutral pions (π^0 bumps). These are in turn produced by interactions of protons with hard X-ray photons (> 50 keV) whose number density can increase during flares. No π^0 bumps are predicted in X-ray "quiescence", as the proton energy is not high enough to exceed the threshold for pion production. We explore the physical conditions needed for the emergence of narrow π^0 bumps in blazar VHE spectra and apply our model to the observations of Mrk 501. We show that the VHE spectrum of Mrk 501 can still be explained by the model, if the energetic photons are provided by an external source of radiation and protons are intermittently accelerated to **a different** region **from** the one producing the X-ray flare itself. We also compute the accompanying TeV muon neutrino flux, and find that this would be hidden in the atmospheric muon background.

7th Heidelberg International Symposium on High-Energy Gamma-Ray Astronomy (Gamma2022)
4-8 July 2022
Barcelona, Spain

*Speaker

PoS(Gamma2022)081

1. Introduction

Blazars are a rare class of active galactic nuclei (AGN) with relativistic jets that are closely aligned to our line of sight [14]. The spectral energy distribution (SED) of blazars can span ~ 15 decades in energy starting from radio frequencies and extending to γ-rays. The flux across the spectrum is variable on different timescales, ranging from minutes to months, with larger variability amplitudes found usually in X-rays and γ-rays [for a review, see 3]. In this contribution we study the emergence of narrow features in VHE γ-ray blazar spectra produced via the decay of neutral pions (π^0 bumps). We focus on high-synchrotron-peaked (HSP) blazars, like Mrk 501, which are often detected at VHE energies [1, 4]. In fact, HSPs are the majority of the ~ 90 extragalactic sources detected at VHE by imaging atmospheric Cherenkov telescopes (see TeVCat catalog[1]). We perform time-dependent numerical calculations to simulate X-ray and VHE γ-ray flares of HSP blazars. We search for conditions leading to the emergence of π^0 bumps in VHE spectra and apply our model to Mrk 501 observations.

2. Model and Methods

To produce TeV γ-ray photons (in the observer's frame) from π^0 decay, the parent proton energy in the comoving frame of the jet should be $\varepsilon'_{\rm p} \approx 1\ {\rm TeV}\ (1+z)\left(\varepsilon_\gamma/1\ {\rm TeV}\right)(\delta/10)^{-1}$, where z is the source redshift and δ is the Doppler factor of the emitting region. The target photons used in photomeson interactions with protons of energy $\varepsilon'_{\rm p}$ should have comoving energy $\varepsilon'_{\rm t} \gtrsim \bar{\varepsilon}_{\rm th} m_{\rm p} c^2/2\varepsilon'_{\rm p}$, where $\bar{\varepsilon}_{\rm th} = m_{\pi^0}c^2(1+m_{\pi^0}/2m_{\rm p}) \simeq 0.145$ GeV.

We assume that relativistic protons interact with X-ray photons produced locally in the jet by non-thermal electrons. For interactions with jet photons the threshold energy condition is written as

$$\left(\frac{\varepsilon_{\rm t}}{0.5\ {\rm MeV}}\right)\left(\frac{\varepsilon_\gamma}{1\ {\rm TeV}}\right) \gtrsim 1.45\ (1+z)^{-2}\left(\frac{\delta}{10}\right)^2. \tag{1}$$

In non-flaring states the maximum proton energy is lower than the one needed for the production of pionic TeV γ-rays. However, during hard X-ray flares with peak energies > 100 keV, the condition can be met by the most energetic protons in the emitting region, leading to the production of pionic γ-rays. **This condition could also be met by relativistic protons interacting with MeV photons in the jets of bright flat spectrum radio quasars (FSRQs), resulting in TeV pionic flares.**

Alternatively, relativistic protons can interact with ambient X-ray photons, e.g. from a disk-corona system or a radiatively inefficient accretion flow. In this case the threshold condition reads

$$\left(\frac{\varepsilon_{\rm t}}{10\ {\rm keV}}\right)\left(\frac{\varepsilon_\gamma}{1\ {\rm TeV}}\right) \gtrsim 1.45\ (1+z)^{-2}. \tag{2}$$

where we used $\varepsilon'_{\rm t} \approx \Gamma\varepsilon_{\rm t}(1+z)$ and $\delta \approx 2\Gamma$. Here, the production of pionic γ-rays happens in a different region than the one producing the bulk of the multi-wavelength flare by non-thermal electrons.

To simulate the π^0 bumps in the VHE spectra of flaring blazars we use the numerical code ATHEνA [5]. This computes the multiwavelength photon and all-flavour neutrino spectra as a

[1] tevcat.uchicago.edu

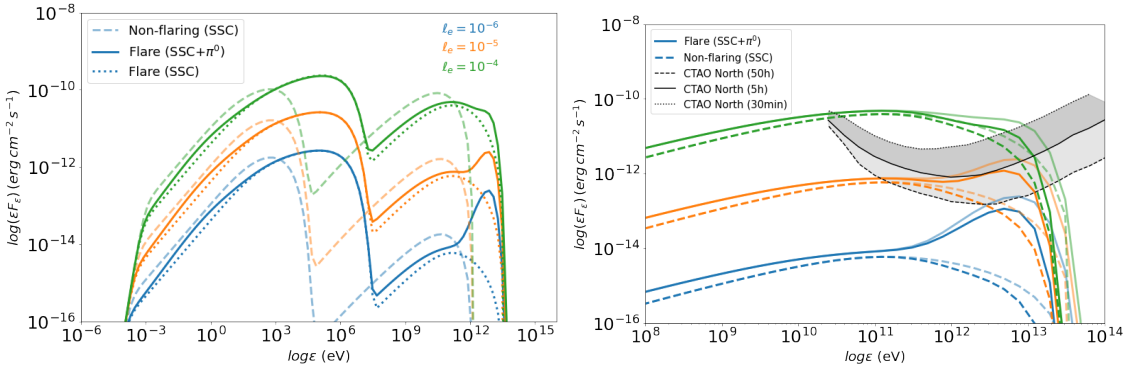

Figure 1: *Left:* Non-flaring and X-ray flaring SEDs computed for three values of the electron compactness ℓ_e as indicated in the plot. Attenuation of VHE γ-rays due to the EBL is not included here. Other parameters used are: $B' = 0.86$ G, $R' = 10^{15}$ cm, $\delta = 20$, $\ell_p = 1$, $s_e = s_p = 1.7$, $\gamma_{e,max} = 10^5$ (pre-flare) and $10^{6.5}$ (flare), $\gamma_{p,max} = (m_e/m_p)\gamma_{e,max}$. *Right*: Zoom in the γ-ray part of the spectra shown on the left panel. Spectra with (without) EBL attenuation are plotted with darker (lighter) colored lines. Here, the EBL model of Franceschini, Rodighiero, & Vaccari [6] was used and a distance of $d_L = 149.4$ Mpc was assumed. Shaded regions indicate the range of sensitivities for the **"Alpha Configuration" of the** CTA Northern Array **(adopted from the CTAO website)** expected for different exposure times (see inset legend).

function of time by solving a set of coupled integro-differential equations for relativistic protons, secondary electrons and positrons, photons, neutrons, and neutrinos using all the relevant radiative processes.

3. Results for a generic blazar

We present results for the case of proton interactions with the jet photons during an X-ray flare. We assume that prior to the onset of an X-ray flare, the blazar SED is fully explained by the SSC radiation of a power-law distribution of relativistic electrons, i.e. $dN_e/d\gamma_e \propto \gamma_e^{-s_e}$, $1 < \gamma_e \leq \gamma_{e,\rm max}$ (see dashed lines in the left panel of Fig. 1). The X-ray flare is simulated by an episodic increase of the maximum electron energy (e.g. $\gamma'_{e,\rm max} = 30\,\gamma_{e,\rm max}$ within the dynamical time). Assuming that protons are accelerated to the same maximum energy as electrons, during the flare they can achieve a high enough $\gamma_{p,\rm max}$ to satisfy the energy threshold for pion production on the electron synchrotron X-ray photons – see Eq. (1). As a result of π^0 decay, the flaring spectra may exhibit a narrow spectral feature or spectral hardening in the VHE band as illustrated by the solid colored lines in Fig. 1. A key parameter that determines the final shape of the VHE spectrum is the ratio of the electron to proton injection luminosities in the flaring emission region. We find that $(L_{\rm SSC+\pi^0}/L_{\rm SSC})_{>1\rm TeV} \propto \ell_p/\ell_e$, where $\ell_{e(p)} = \sigma_T\, L_{e(p)}/(4\pi R' \delta^4 m_{e(p)} c^3)$ and R' is the radius of the spherical emitting region. On the right panel of Fig. 1 we compare the predicted VHE flaring spectra (with SSC and π^0 contributions) of a hypothetical blazar at the distance of Mrk 501 (149.4 Mpc) with the projected differential sensitivity of the Cherenkov Telescope Array (CTA) for different exposure times (as noted on the inset legend). For the brightest flare (green colored curves) CTA would be sensitive to probe a transient π^0 bump at about 10 TeV even with an 1 hr exposure.

4. Application to Mrk 501

Mrk 501 is an HSP blazar at $z = 0.034$ that is well known for its X-ray and VHE flaring activity. It is also characterized as a transient extreme blazar. **MAGIC Collaboration** [12] reported the results of a multi-wavelength campaign performed in July 2014. For a period of about two weeks, Mrk 501 exhibited the highest X-ray activity ever detected by *Swift* during its operation. VHE flaring activity correlated with the X-rays was also recorded. Moreover, a narrow feature at ~ 3 TeV was detected at a significance level of about 4σ in the VHE spectrum measured with the MAGIC telescopes on 2014 July 19 (MJD 56857.98). This feature is inconsistent with the empirical functions typically used to describe VHE blazar spectra, i.e. power law, log-parabola, log-parabola with exponential cutoff. In this case, the typical one-zone SSC model fails to explain the VHE spectrum **and more complex scenarios are needed [for alternative leptonic scenarios, see 12].**

We applied the model (with pion production on X-ray jet photons) to the data of Mrk 501 (MJD 56857.98), assuming the *Swift*-BAT data are consistent with a peak synchrotron of 500 keV. We found that the superposition of the SSC and the π^0 components produces a broader spectral feature than the one observed with MAGIC. Therefore, this variant of the model is disfavored for the specific dataset. These results will be presented in Petropoulou et al. (in prep). Here, we test the alternative scenario outlined in Sec. 2: an injection episode of relativistic protons takes place into a compact region of the jet that is embedded in an isotropic ambient X-ray photon field (Zone 1). X-rays could originate from a hot corona or from the accretion flow itself. Relativistic electrons, injected in a more extended region of the jet (Zone 2), emit SSC radiation producing the bulk of the multi-wavelength spectrum of the flare.

The majority of BL Lacs, like Mrk 501, are thought to be powered by radiatively inefficient disks accreting at sub-Eddington rates [e.g. 7]. Synchrotron radiation from hot thermal electrons in the disk produces infrared and radio emission; hard X-rays and soft γ-rays (up to a few MeV) can naturally arise from Comptonization in the disk. Here, we adopt the spectral template of a radiatively inefficient accretion disk (RIAF) computed by [11] for various accretion rates. In our calculations we adopt the spectrum for $\dot{m} = 0.01$, which is the mean of the logarithmic accretion rates estimated by [15] using a sample of 43 BL Lacs. It is further assumed that the RIAF radiation is scattered elastically by gas clouds located at a distance $R_{\rm ext}$, producing an almost isotropic photon field within a sphere of $R_{\rm ext}$ with the same spectrum as that of incident radiation. We set $R_{\rm ext} = 10^{16}$ cm, which corresponds to ~ 34 Schwarzschild radii for a black hole mass $M = 10^9 M_\odot$ [2]. Therefore, a blob of radius $R' = 10^{15}$ cm in a conical jet with $\Gamma = 10$ can be embedded in this ambient radiation field. The energy density of external photons as seen in the blob rest frame is $u'_{\rm ext} \approx \Gamma^2 L_{\rm ext}/(4\pi R_{\rm ext}^2 c)$, where $L_{\rm ext}$ is the luminosity of the external field, which is taken from [11]. Finally, the proton injection compactness is modeled with a Lorentzian function in time that has a full width at half maximum $\Delta T_{1/2} \simeq 2.3$ hr (in the observer's frame) and a peak value of $\ell_{\rm p,pk} = 1.3$. All parameter values used are summarized in Table 1.

The model spectra computed in this scenario are presented in Fig. 2 (left and middle panels). Colored solid lines show the temporal evolution (see also color bar) of the hadronic cascade (HC) spectrum produced in Zone 1. Note that the total duration of the simulated flare is about 7.7 hr, while the LAT data adopted from [12] were averaged over a larger time window (4 and 10 days). Protons of comoving energy ~ 1.6 TeV interact with the external photons (whose density and energy

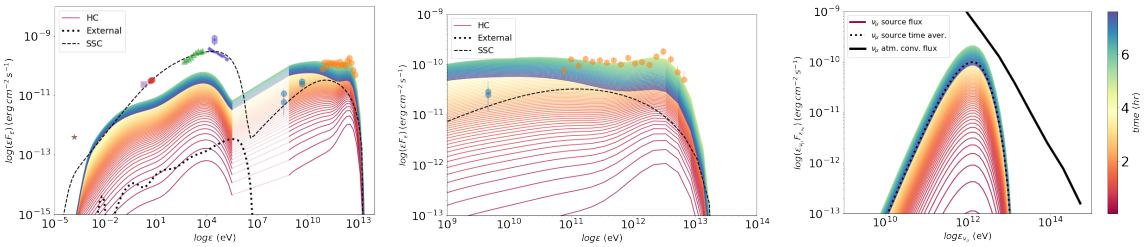

Figure 2: *Left panel:* SED of Mrk 501 on MJD 56857.98 compiled using the data from [12]. Solid colored lines show the evolution of the hadronic cascade (HC) emission produced in a compact jet region (Zone 1), while the dashed black line shows the SSC emission from a more extended jet region (Zone 2). The broadband spectrum of the external radiation field is that of a RIAF disk [adopted from 11] – see dotted black line. Transparency is used for the energy range where interpolation of the simulated HC spectra is necessary due to coding implementation. *Middle panel:* Zoom in the γ-ray spectrum. The HC and SSC combined spectrum describes well the MAGIC data. *Right panel:* Snapshots of the $\nu_\mu + \bar{\nu}_\mu$ energy flux spectrum at different times (indicated by different colors) produced in Zone 1. The time-average spectrum is overplotted for comparison (dotted black line). The thick black line shows the energy spectrum of the atmospheric neutrino flux based on the HKKMS2007 model for an observational window size of 1 degree (adopted from [9]). The color bar is common for all three panels.

Table 1: Parameter values used in the SED model of Mrk 501 presented in Fig. 2.

Zone 1		Zone 2		External photons	
Parameter	Value	Parameter	Value	Parameter	Value
δ	12	δ	12	$\dot{m}$	10^{-2}
R' (cm)	10^{15}	R' (cm)	2×10^{16}	$R_{\rm ext}$ (cm)	10^{16}
B' (G)	1	B' (cm)	0.2	$L_{\rm ext}$ (erg s^{-1})	4.9×10^{42}
$\ell_{\rm p,pk}$	1.3	$\ell_{\rm e}$	$10^{-4.4}$		
$s_{\rm p}$	2.0	$s_{\rm e}$	1.6		
$\gamma'_{\rm p,min}$	$10^{3.0}$	$\gamma'_{\rm e,min}$	1		
$\gamma'_{\rm p,max}$	$10^{3.2}$	$\gamma'_{\rm e,max}$	$10^{6.5}$		
$\Delta T_{1/2}$ (hr)	2.3				

appear boosted in the comoving frame) producing secondary pairs and pionic γ-rays. Notice the clear signature of the π^0 decay peaking at $\sim$ 2.4 TeV. Depending on the density of low-energy photons in Zone 1, a fraction of the VHE γ-rays is attenuated, thus leading to the production of more secondary pairs.

The cascade emission that we show in Fig. 2 is the combined result of synchrotron and inverse Compton radiation of relativistic pairs produced via photopair, photomeson and $\gamma\gamma$ pair production processes[2]. Finally, the SSC emission from Zone 2 is overplotted with a dashed black line. This should be added to the HC emission to produce the total spectrum at any given time (not shown explicitly). For the selected parameters, pairs are radiating more efficiently via inverse Compton scatterings, hence the cascade emission is Compton-dominated, and produces a broad peak in the GeV band. A stronger magnetic field in Zone 1 would channel the energy of pairs to the lower end of the spectrum, as these would cool preferentially via the synchrotron process. Therefore, the magnetic field of Zone 1 can be constrained by observations in the infrared and optical bands to

[2]Proton interactions with their own cascade emission are also included in our calculations.

< 10 G.

In Fig. 2 (right panel) we also present the model-predicted muon neutrino spectra during the evolution of the VHE flare. The $\nu_\mu + \bar{\nu}_\mu$ neutrino energy fluxes are obtained after taking into account neutrino mixing due to oscillations. The neutrino and γ-ray spectra from π^0 decays are very similar, with the former being shifted in energy by a factor of two [10]. As a result, the predicted peak neutrino flux is comparable to the flux of the narrow spectral feature seen at ~ 3 TeV in the VHE spectrum of Mrk 501. Despite the high peak neutrino energy flux, detection of an astrophysical signal from a point source at TeV energies might be hampered by the large atmospheric neutrino flux, **which is considered a background for astrophysical neutrino searches. The atmospheric neutrino spectrum is soft, and** can be approximated by $F_{\varepsilon_\nu}/\varepsilon_\nu \propto \varepsilon_\nu^{-3.7}$ [HKKMS2007, 8].

The conventional atmospheric muon neutrino flux (based on HKKMS2007) is overplotted (solid black line) for comparison. The spectrum is adopted from [9] after assuming a constant flux across a small observational window size of 1^o [see also 13]. The source neutrino flux stays below the background for the duration of the flare. Nonetheless, if pion-like bumps similar to that of Mrk 501 were to be discovered at higher energies (e.g. at 10 TeV), the prospects of detecting neutrinos during VHE flares would be improved.

5. Conclusions

We have investigated the production of narrow spectral features in the VHE spectra of flaring blazars due to π^0 decay. We have shown that CTA will be sensitive to detect π^0 bumps or spectral hardening not expected in the standard SSC model even up to 10 TeV for nearby blazars. Future searches for atypical features in the VHE spectra of X-ray flaring HSPs are strongly motivated, as they can probe the otherwise hidden relativistic hadronic population of the jet.

References

[1] Abe H., Abe S., Acciari V. A. et al., 2022, arXiv, arXiv:2210.02547
[2] Barth A. J., Ho L. C., Sargent W. L. W., 2002, ApJL, 566, L13.
[3] Böttcher M., 2019, Galax, 7, 20.
[4] Chang Y.-L., Arsioli B., Giommi P., Padovani P., Brandt C. H., 2019, A&A, 632, A77.
[5] Dimitrakoudis S., Mastichiadis A., Protheroe R. J., Reimer A., 2012, A&A, 546, A120.
[6] Franceschini A., Rodighiero G., Vaccari M., 2008, A&A, 487, 837.
[7] Ghisellini G., Tavecchio F., Foschini L., Ghirlanda G., 2011, MNRAS, 414, 2674.
[8] Honda M., Kajita T., Kasahara K., Midorikawa S., Sanuki T., 2007, PhRvD, 75, 043006.
[9] IceCube Collaboration, Aartsen M. G., Ackermann M., Adams J., Aguilar J. A., Ahlers M., Ahrens M., Altmann D., et al., 2015, PhRvD, 91, 122004.
[10] Kelner S. R., Aharonian F. A., 2008, PhRvD, 78, 034013.
[11] Kimura S. S., Murase K., Mészáros P., 2021, NatCo, 12, 5615.
[12] MAGIC Collaboration, Acciari V. A., Ansoldi S., Antonelli L. A., Babić A., Banerjee B., Barres de Almeida U., et al., 2020, A&A, 637, A86.
[13] Petropoulou M., Coenders S., Dimitrakoudis S., 2016, APh, 80, 115.
[14] Urry C. M., Padovani P., 1995, PASP, 107, 803.
[15] Wang J.-M., Staubert R., Ho L. C., 2002, ApJ, 579, 554.